# Kontrolle rauschinduzierter Oszillationen im Van-der-Pol-Modell

## Analyt. Näherung der spektralen Leistungsdichte:

Fourier-Trafo der mean-field-Gln $\dot{x} = y$

$$\dot{y} = \tilde{\varepsilon} y - \omega_0^2 x + D\xi(t) + K[y(t-\tau) - y(t)]$$

$$x(t) = \int_{-\infty}^{\infty} d\omega\, e^{-i\omega t}\, \hat{x}(\omega)$$

$$-i\omega \hat{x}(\omega) = \hat{y}(\omega)$$

$$-i\omega \hat{y}(\omega) = \tilde{\varepsilon}\hat{y}(\omega) - \omega_0^2 \hat{x}(\omega) + D\hat{\xi}(\omega) + K\hat{y}\left(e^{i\omega\tau} - 1\right)$$

Elim. von $\hat{x}(\omega) = \frac{i}{\omega}\hat{y}(\omega)$:

$$-i\omega\hat{y} - \tilde{\varepsilon}\hat{y} + i\frac{\omega_0^2}{\omega}\hat{y} - K\left(e^{i\omega\tau} - 1\right)\hat{y} = D\hat{\xi} \qquad | \cdot i\omega$$

$$\hat{y}(\omega) = \frac{i\omega D\hat{\xi}(\omega)}{\omega^2 - \omega_0^2 - i\omega\tilde{\varepsilon} - i\omega K\left(e^{i\omega\tau} - 1\right)}$$

$$\langle \hat{y}(\omega)\hat{y}^*(\omega')\rangle = \frac{(i\omega D)(-i\omega' D)\langle \hat{\xi}(\omega)\hat{\xi}^*(\omega')\rangle}{(\omega^2 - \omega_0^2 - i\omega[\tilde{\varepsilon} + K(e^{i\omega\tau} - 1)])(\omega'^2 - \omega_0^2 + i\omega'[\tilde{\varepsilon} + K(e^{-i\omega'\tau} - 1)])}$$

$$\langle \hat{\xi}(\omega)\hat{\xi}^*(\omega')\rangle = \frac{1}{(2\pi)^2}\int_{-\infty}^{\infty} dt\, e^{i\omega t}\int_{-\infty}^{\infty} dt'\, e^{-i\omega' t'}\underbrace{\langle \xi(t)\xi(t')\rangle}_{\delta(t-t')}$$

$$= \frac{1}{2\pi}\underbrace{\frac{1}{2\pi}\int_{-\infty}^{\infty} dt\, e^{i(\omega-\omega')t}}_{\delta(\omega-\omega')}$$

$$\omega = \omega' \Rightarrow \langle \hat{y}(\omega)\hat{y}^*(\omega')\rangle = \frac{D^2}{2\pi}\frac{\omega^2\,\delta(\omega-\omega')}{\left(\omega^2 - \omega_0^2 + \omega K\sin\omega\tau\right)^2 + \omega^2\left\{\tilde{\varepsilon} - K(1-\cos\omega\tau)\right\}^2}$$

Wiener - Khinchine - Theorem:

$$\langle \hat{y}(\omega)\,\hat{y}^*(\omega')\rangle = \frac{1}{(2\pi)^2}\int_{-\infty}^{\infty} dt\, e^{i\omega t}\int_{-\infty}^{\infty} dt'\, e^{-i\omega' t'}\,\langle y(t)\,y(t')\rangle \qquad t+s$$

$$= \underbrace{\frac{1}{2\pi}\int_{-\infty}^{\infty} dt\, e^{i(\omega-\omega')t}}_{\delta(\omega-\omega')}\;\underbrace{\frac{1}{2\pi}\int_{-\infty}^{\infty} ds\, e^{i\omega'\underbrace{(t-t')}_{-s}}\,\langle y(t)\,y(t+s)\rangle}_{S(\omega')}$$

$$\Rightarrow S_{yy}(\omega) = \frac{D^2}{2\pi}\,\frac{\omega^2}{(\omega^2-\omega_0^2+\omega K\sin\omega\tau)^2+\omega^2(\tilde{\varepsilon}-K(1-\cos\omega\tau))^2}$$

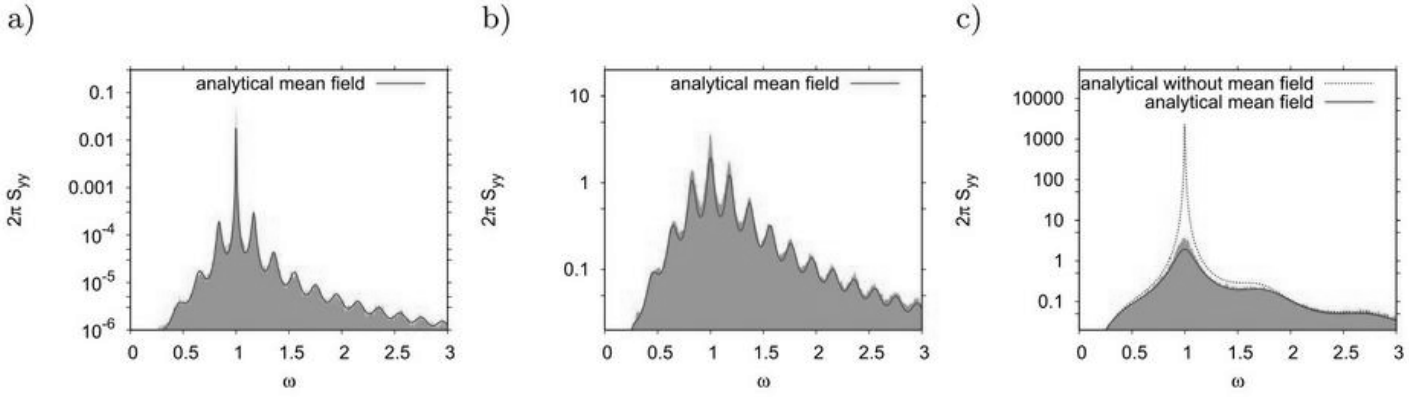


Fig. 4 – Spectrum $S_{yy}(\omega)$ for the VdP system in the presence of delayed feedback for $\varepsilon = -0.01$, $K = 0.2$: a) $D = 0.003$, $\tau = 31.4$; b) $D = 0.5$, $\tau = 31.4$; c) $D = 0.5$, $\tau = 6.3$. Shaded: numerically simulated spectra; solid line: spectrum estimated analytically by (19); dashed line in c): spectrum estimated analytically without mean field ($\tilde{\varepsilon} = \varepsilon$) [14].

Pomplun et al, Europhys. Lett

hervorragende Übereinstimmung der mean-field-Näherung mit der vollen nichtlin. Simul. der Dgl., sogar für große D

$K=0$: $$S(\omega) = \frac{D^2}{2\pi}\,\frac{\omega^2}{(\omega^2-\omega_0^2)^2+\omega^2\tilde{\varepsilon}^2}$$

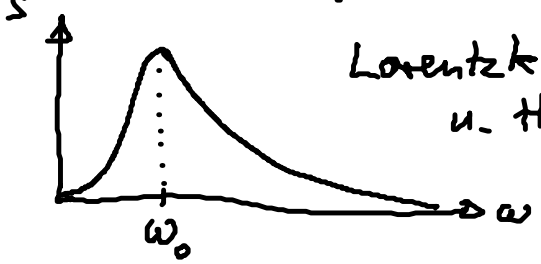


Lorentzkurve mit Max. bei $\omega_0$
u. Halbwertsbreite $\approx \frac{|\tilde{\varepsilon}|}{2} = \frac{2}{\pi t_{cor}}$

$K \neq 0$: immer mehr Nebenmax. mit zunehmendem $\tau$

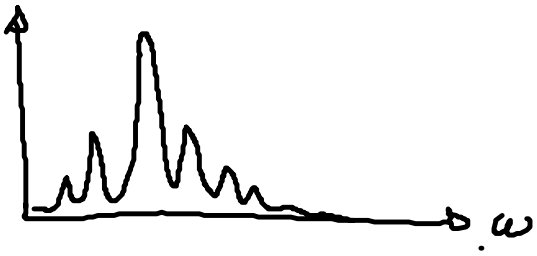


## generisches Modell für Anregbarkeit Typ I

(knapp unterhalb der SNIPER-Bifurkation)

Arnst, Hövel, Hizanidis, Schöll, Eur. Phys. J. - ST, submitted 9.6.10

$$\dot{x} = x(1-x^2-y^2) + y(x-b) + D\xi(t) + K[x(t-\tau) - x(t)]$$
$$\dot{y} = y(1-x^2-y^2) - x(x-b) + D\xi(t) + K[y(t-\tau) - y(t)]$$

$K=D=0$ $b<1$ : stab. Fixpkt (Knoten), anregbares Regime

$b=1$ : Sattel-Knoten-Bif. auf Grenzzyklus $r=1$, $T\to\infty$

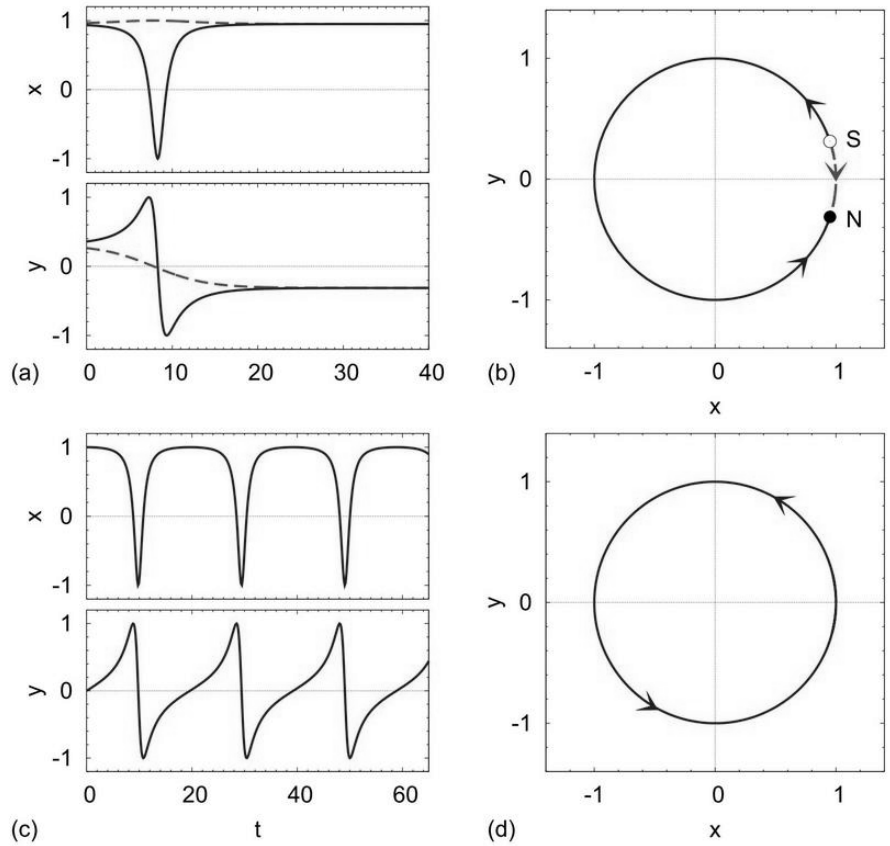


**Fig. 1.** (Color online) Time series (a),(c) and phase portraits (b),(d) of the analytic solutions of Eqs. (2). Panels (a),(b) refer to $b = 0.95 < 1$ with analytic solutions given by Eq. (7); full (blue) and broken (red) lines refer to two different initial conditions. Panels (c),(d) correspond to $b = 1.05 > 1$, see Eq. (8). ($K = D = 0$)

D = 0 : Delay-induzierte globale (homokline) Bifurk.

Hizanidis et al., Int. J. Bif. Chaos 18, 1759 (2008)

Fixpkt. N (node) bleibt immer stabil, aber homokline Bif.  eines stab. Grenzzyklus, r>0, T→∞




Fig. 2. (a) Two-dimensional projection of the phase space below the homoclinic bifurcation ($K = 0.335$). (b) Homoclinic orbit (red) achieved at $K_c = 0.3401$. (c) Delay-induced limit cycle (red) above the homoclinic bifurcation ($K = 0.3438$). (d) Scaling of the oscillation period $T$ above but close to the critical point $K_c$ (crosses: simulation data, solid line: linear fit). Full and open circles mark stable and unstable fixed points, respectively. Parameters: $b = 0.95$, $\tau = 3$.

Bifurkations-diagramm ($D=0$)

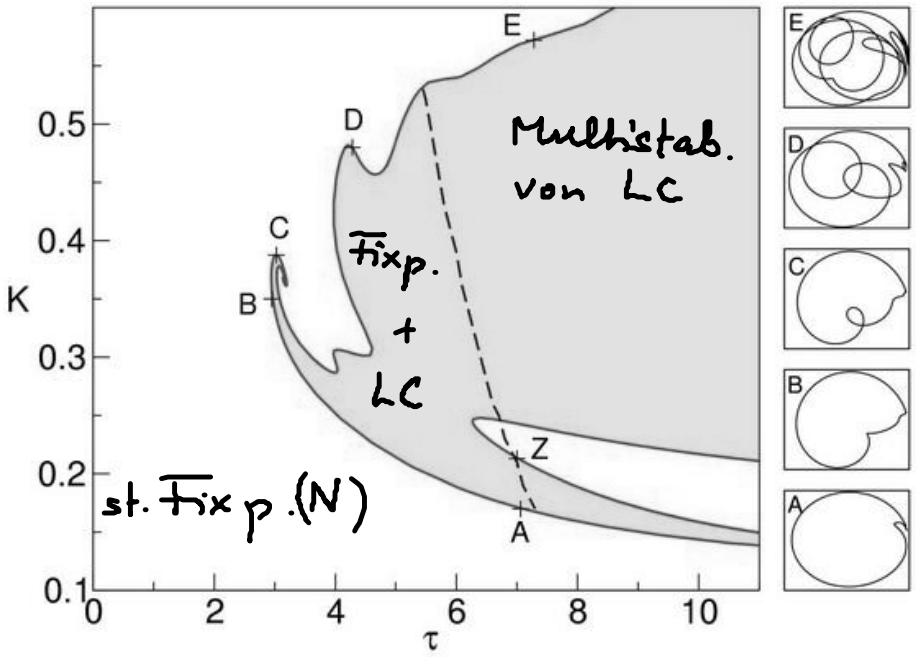


Fig. 3. Curve of homoclinic bifurcations (red) in the $K$–$\tau$ plane (left). A–E labels various points with homoclinic orbits, which are shown in the $x$–$y$ phase plane in the panel on the right. Delay-induced limit cycles exist, in addition to the stable fixed point, in the yellow area. The blue dashed curve separates the regions $\sigma_0 < 0$ (left) and $\sigma_0 > 0$ (right).

Shilnikov-Theorie

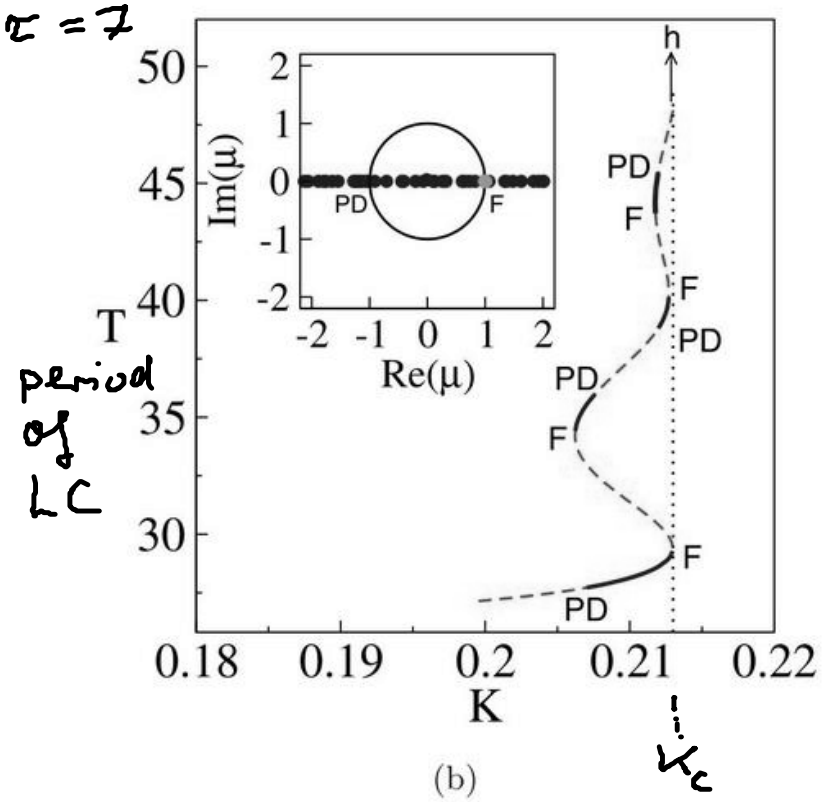


Fig. 5. (a) Period $T$ of limit cycle born in a homoclinic bifurcation at $(K, \tau) = (0.17145, 7)$ (point A in Fig. 3, $\sigma_0 < 0$). (b) Period $T$ of limit cycles in the multistable regime at $(K, \tau) = (0.213, 7)$ (point Z in Fig. 3, $\sigma_0 > 0$), undergoing

infinitely many fold (F) and period-doubling (PD) bifurcations, before ending in a homoclinic orbit h for $T \to \infty$ at $K = 0.213$. Solid blue and red dashed lines denote stable and unstable limit cycles, respectively. The insets show the two leading Floquet multipliers of the periodic orbit $\mu_1 = 1$ (green) and $\mu_2$ (blue) with $K$ as a parameter in (a), and $T$ as a parameter in (b), in the complex plane $b = 0.95$.

$D \neq 0$ : Kontrolle rauschinduzierter und rauschbeeinflusster Oszillationen

↓

delay-induzierte deterministische Grenzzyklen

- Kohärenzresonanz (für $K=0$) wird verstärkt durch zeitverzögerte Rückkopplungskontrolle

Ansatz et al (2010)

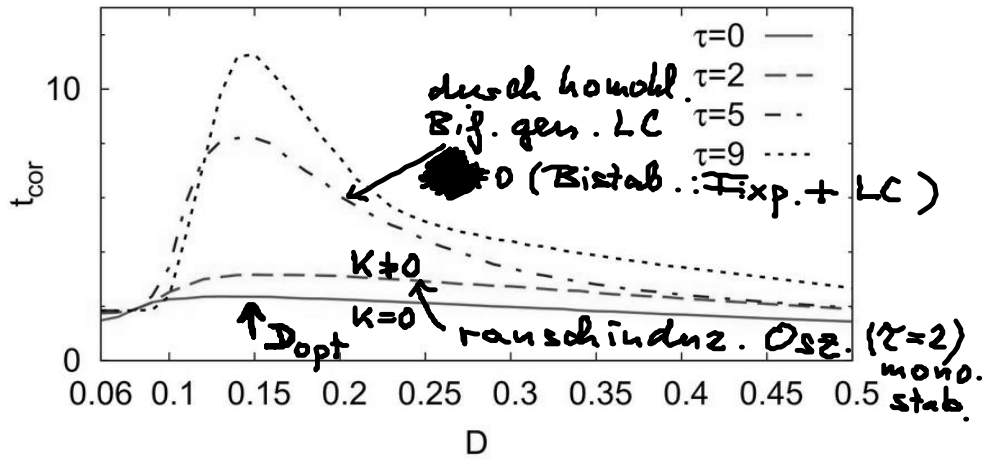


**Fig. 4.** (Color online) Correlation time in dependence on the noise intensity $D$ for different time delays $\tau$. The solid (green) curve corresponds to the uncontrolled system ($\tau = 0$). The dashed (red), dash-dotted (blue), and dotted (black) curves refer to values of $\tau = 2, 5$, and 9, respectively. Other parameters: $b = 0.95$ and $K = 0.25$.

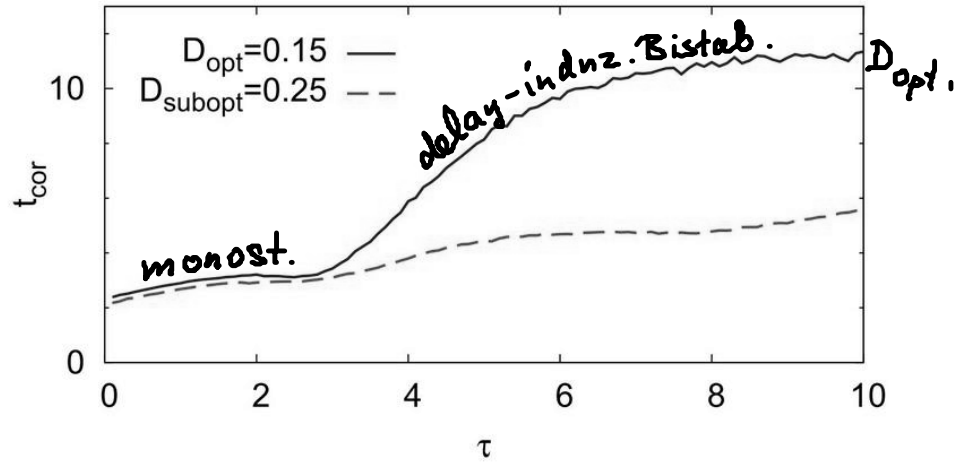


**Fig. 5.** (Color online) Correlation time $t_{cor}$ in dependence on the time delay $\tau$ for two values of the noise intensity $D$. The dashed (red) curve corresponds to $D_{subopt} = 0.25$ and the solid (blue) curve refers to $D_{opt} = 0.15$. Other parameters: $b = 0.95$ and $K = 0.25$.

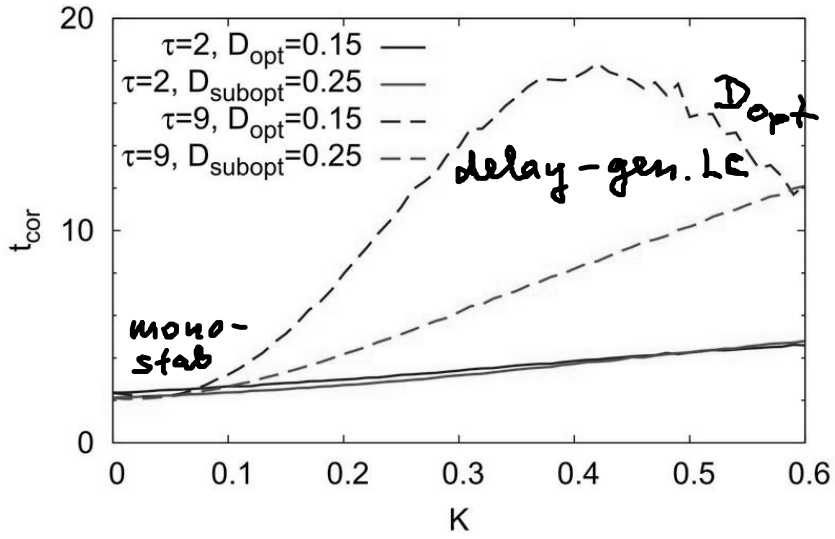


**Fig. 6.** (Color online) Correlation time $t_{cor}$ in dependence on the control strength $K$ for two values of the noise intensity $D$ and two values of the delay time $\tau$. The gray (red) and black (blue) curves depict the cases of $D_{subopt}$ and $D_{opt}$, respectively. The solid and dashed lines correspond to $\tau = 2$ and $\tau = 9$, respectively. Other parameter: $b = 0.95$.